[3] Sergre, S. E. and Allen, T. E., "Magnetic probes of high frequency response," J. Sci. Instr. **37**, 369–371 (1960).

[4] Gooding, T. J., Hayworth, B. R., and Lovberg, R. H., "Instabilities in a coaxial plasma gun," AIAA J. **1**, 1289–1292 (1963).

[5] Jahn, R. G. and von Jaskowsky, W., "Structure of a large-radius pinch discharge," AIAA J. **1**, 1809–1814 (1963).

[6] Burkhardt, L. C. and Lovberg, R. H., "Current sheet in a coaxial plasma gun," Phys. Fluids **5**, 341–347 (1962).

[7] Gloersen, P., "Pulsed plasma accelerators," ARS Preprint 2129-61 (October 1961).

[8] Guman, W. J., "Dynamic behavior of nonsteady axisymmetric magnetically driven slug-type plasma sheets," Ph.D. Thesis, Dept. Aeronaut. Eng., Rensselaer Polytechnic Inst. (1963).

[9] Hart, P. J., "Plasma acceleration with coaxial electrodes," Phys. Fluids **5**, 38–47 (1962).

[10] Gooding, T. J., Hayworth, B. R., and Lovberg, R. H., "Physical processes in a coaxial plasma gun," AIAA Preprint 63004 (March 1963).

[11] McIlroy, W. and Siegel, B., "Analysis of factors influencing plasma engine performance," Am. Soc. Mech. Engrs. Hydraulics, Gas Turbine, Aviation and Space Meeting, Los Angeles (March 3–7, 1963).

[12] Michels, C. J. and Ramins, P., "Performance of coaxial plasma gun with various propellants," International Symposium on Plasma Coaxial Guns, Cleveland (September 6–7, 1962).

[13] Keck, J., "Current speed in a magnetic annular shock tube," Avco-Everett Research Lab., Res. Rept. 152 (May 1963).

[14] Steinberg, A. and Levy, G., "Determination of pinch plasma engine exhaust profiles by microwave interferometry techniques," Inst. Electrical Engrs. International Convention, New York (March 25–28, 1963).

NOVEMBER 1963 AIAA JOURNAL VOL. 1, NO. 11

Conductivity Probe Measurements in Flames

R. A. Olson* and E. C. Lary†
United Aircraft Corporation, East Hartford, Connecticut

An electrodeless probe has been developed to measure the electrical conductivity of high-temperature gases or flames. The weak interaction of an rf field with a plasma is employed to measure the conductivity in the immediate vicinity of the probe. The probe overcomes the principal difficulties associated with techniques employing electrodes or microwaves and is generally applicable to subsonic flows. Values of conductivity in the range of 0.04 to 0.27 mho/m have been detected with the probe in traversing an alkali-seeded hydrogen-oxygen flame. The same probe has shown a linear response to the conductivity of electrolytic solutions of up to 40 mho/m.

Introduction

SEVERAL techniques have been advanced for measuring the electrical conductivity of flames. The most common techniques have difficulties associated with the use of electrodes, including the effects of boundary layers, electrical sheaths, contact potentials, and thermionic emission.[1] These difficulties have been overcome in several investigations by the use of an electrodeless interaction with the flame. Williams[2] employs a resonant coil surrounding the flame to obtain a relative measurement of dissipation in the flame. The primary difficulty here is that only an average measurement over a large region of the flame can be obtained and that absolute values of conductivity were not obtained. Microwave techniques used by still other investigators (e.g., Ref. 3), though having many advantages, involve an average of the interaction over the entire path length through the flame.

A conductivity measurement probe has been developed in order to overcome difficulties in the measurement of plasma conductivity in MHD devices.[4] The probe detects the conductivity in its immediate vicinity by dissipating a very small amount of rf power in the plasma. The weak interaction with the plasma is detected by observing the resistive loading of a sensitive rf oscillator-detector. Ring currents are induced in the plasma, about the insulated probe, so that the difficulties associated with electrodes are eliminated. Moreover, the measuring frequency of about 20 Mc/sec is well below the electron collision frequency of the flame, insuring that the d.c. electrical conductivity is measured by the rf probe.

The electrodeless probe technique has been applied to the measurement of the conductivity of electrolytes, semiconductors, low-density plasmas (including rf discharge plasmas), and the high-temperature ionized-gas flow of an MHD generator. More recently, the technique has been employed in the measurement of flame conductivity. This application required a miniaturization of the probe, as well as improved instrumentation, in order to detect and resolve very small values of conductivity. At the same time, a simplification of the probe design (with the elimination of the need for cooling) was achieved by traversing the probe very quickly through the flame. The outer shell of the probe is an insulator, thereby eliminating spurious thermal effects during the period of probing.

Conductivity Measurement Probe

The conductivity probe is basically a single-layer, tightly wound helical coil impressed with rf currents by an external circuit. The coil acts as the primary of an rf transformer in which the plasma is a short-circuited secondary that dissipates a small amount of power. The coil produces an

Presented at the ARS Ions in Flames and Rocket Exhausts Conference, Palm Springs, Calif., October 10–12, 1962; revision received August 23, 1963. The authors wish to express their gratitude to several colleagues for their helpful efforts; especially to A. Witherell for the careful development and construction of the conductivity probes and experimental apparatus, to A. Kozubal for the design of the rf instrumentation, and to W. Price for the microwave measurements. The authors also wish to thank Irvin Glassman of Princeton University for suggesting this application of the conductivity probe.

* Research Scientist, Magnetohydrodynamics, Research Laboratories.

† Principal Scientist, Magnetohydrodynamics, Research Laboratories.

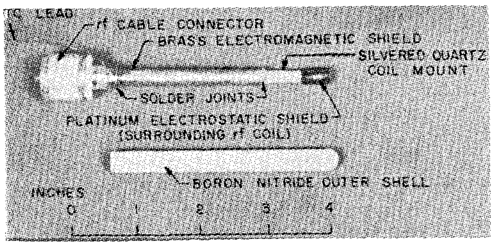

Fig. 1 Conductivity measurement probe.

approximately dipolar magnetic field about the probe, the time variation of which gives rise to an electric field E_θ about the axis of the probe. In the presence of a medium of uniform conductivity σ, an amount of power σE_θ^2 is dissipated per unit volume due to the induced azimuthal current. For sufficiently small values of σ, the rf field will penetrate through the plasma without appreciable (skin effect) attenuation but will decay algebraically according to the rf dipolar magnetic field. Thus, the rf field is not greatly affected by the conducting medium, especially near the probe where E_θ is greatest. The total power dissipation, equal to the integral of σE_θ^2 over the volume of the medium, will therefore be simply proportional to σ. (This regime is called the small R_m regime,[4] in which a distortion of the electromagnetic field does not occur on the length scale of the probe.)

The rf frequency is chosen to be considerably lower than the average electron collision frequency, so that many collisions will occur during a period of oscillation, and the d.c. electrical conductivity will be measured. It is equally important that the measuring frequency avoid the plasma resonance frequency, the electron cyclotron frequency (associated, for example, with an applied magnetic field), and any frequency characteristic of the flow of the conducting medium past the probe. Moreover, any flow past the probe must be subsonic in order to avoid shock waves and the resulting spatial variations of conductivity.

In addition to the coil, the probe (Fig. 1) consists of an electrostatic shield surrounding the coil, the function of which is to prevent the penetration of any axial component E_z into the medium, an electromagnetic shield along the length of the probe, and an insulating shell enclosing the coil and its shielding. The coil leads are returned as a coaxial cable formed by the electromagnetic shield and a central lead along the axis of the probe. The internal temperature of the probe may be monitored with a thermocouple junction at the coil. The probe stem is fabricated of 5-mm quartz tubing, the coil of AWG 32 copper wire, and the shell of high-density boron nitride. The electrostatic and electromagnetic shields are of fired-on platinum and silver, respectively, with the latter being connected through a brass sleeve to a standard coaxial cable fitting at the butt of the probe.

A variety of circuits have been employed to produce the rf signal and to detect the amount of dissipation. The simplest circuit, involving the direct coupling of the probe to a commercial grid-dip meter, is adequate for the measurement of the conductivities in the range of 1 mho/m and above and has the property that the grid current response is approximately linear with conductivity in a large range. More sensitive oscillator-detector circuits that have been developed especially for use with the probe will accurately detect conductivities as low as 0.04 mho/m.

The circuit shown in Fig. 2 represents a stationary oscillator-detector unit that is connected to a movable probe by a flexible coaxial cable. The oscillator, shown at the left, consists of two tubes, one a grounded-grid amplifier that excites the resonant circuit of the probe and the other a cathode follower driving the grounded-grid amplifier. The voltage on the resonant circuit is delivered to the cathode follower to complete the feedback loop. The cathode follower operates in a nonlinear range so that the amplitude of the oscillation determines the average plate current and, hence, plate voltage. The plate voltage of the cathode follower is at a level of about 100 v, with the perturbation signal due to dissipation being of the order of millivolts. The change in plate voltage is amplified in the differential amplifier, shown on the right, with the output (of the order of volts) being detected by a voltmeter. Alternatively, the voltage change due to conductivity was detected at high speed using an oscilloscope, with the meter removed from the circuit. The data described in the subsequent section were obtained by the latter method, using a Tektronix type Z preamplifier and a scope camera to record data.

The values of components in the oscillator and amplifier were selected to provide fast response, with a resulting over-

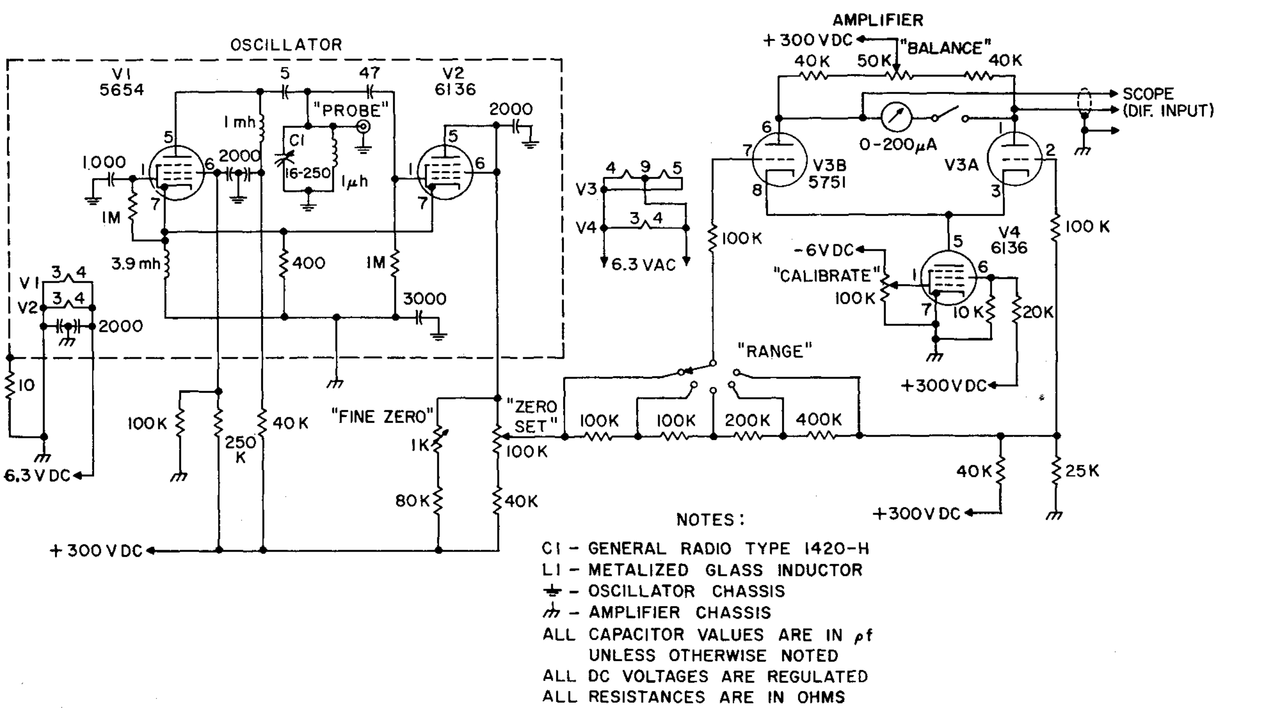

Fig. 2 Diagram of oscillator-detector circuit.

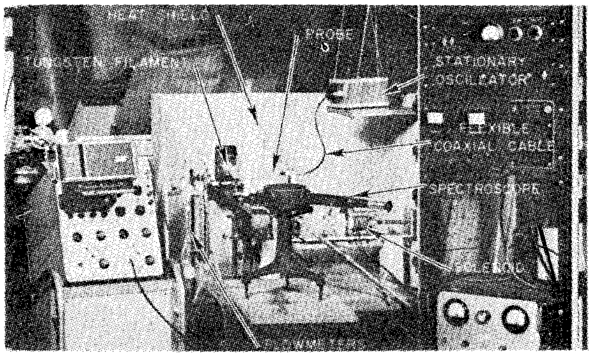

Fig. 3 Stationary oscillator with flexible probe connector.

all response time of about 2 msec. The oscillator was entirely enclosed in a shielding box of $\frac{1}{2}$-in.-thick welded aluminum plates with removable top and bottom covers. The variable capacitor C-1 is a General Radio, type 1420-H, and was provided for frequency control of the resonant circuit. "Zero" and "range" controls were provided as shown in the schematic to control the level of the d.c. output signal. The arrangement of oscillator and movable probe with coaxial cable connection is shown in Fig. 3. A typical probe coil employed in conjunction with the oscillator consisted of 20 turns of AWG 32 copper wire, coaxial with the probe, and of 0.160-in. i.d.

The probes were calibrated with electrolytic solutions of known conductivity. Distilled water gave no detectable signal on the most sensitive scale, and the calibration indicated a linearity of the output signal with conductivity throughout the range of calibration, which extended from zero to 40 mho/m. The calibration with ionic solutions is valid for plasmas and other electronic conductors since the radio frequency is much smaller than the appropriate collison frequency in either case, so that a d.c. measurement is made. The validity of the calibration with electrolytic solutions is exhibited experimentally by the good agreement obtained between conductivity probe measurements in solutions and in a glow discharge plasma, as shown in Fig. 10 of Ref. 4. The glow discharge data agreed well with the electrolytic calibration data except for a constant displacement that has subsequently been eliminated by electrostatic shielding of the probe.

Application to Flame Measurement

The probe was traversed through the flame on a solenoid-actuated sliding mount, shown in Fig. 3. The resulting deformation of the coaxial cable gave a negligible output signal. Because of the high sensitivity required, the data of this section were obtained by manual operation of the traversing mechanism in order to eliminate noise in the signal due to acoustical vibrations. Thermal effects due to traversing the flame gave a spurious signal with a thermal time constant of 78 sec (Fig. 4). The oscilloscope traces obtained in the actual conductivity measurement, shown in Fig. 5, show no thermal effect during the traverse of the probe, which was a period of about 0.3 sec.

A hydrogen-oxygen flame was studied, with and without seeding solutions of alkali chlorides (including NaCl, KCl, RbCl, and CsCl). The torch used throughout was a Bethlehem bench burner (PM2D model A), giving a flame thickness of about 1 in. The addition of seeding solutions was achieved with a glass atomizer that was constructed to yield sufficient seeding concentrations and oxygen throughputs.

The over-all configuration of the experiment is shown in Fig. 3. Flowmeters were provided for measuring the oxygen and fuel flow rates. The seeding solution was added directly to the oxygen flow of both the inner and outer burner ports. The flame temperature for the constant operating conditions selected was found to be 2600°K, as measured by the sodium D-line reversal technique. The temperature of the tungsten filament used for comparison was calibrated using an optical pyrometer.

A uniform region of the flame occurring about 3 in. above the primary reaction zone was studied throughout. The probe was pulsed through the flame and returned to the starting point behind a heat shield that minimized thermal effects prior to pulsing the probe, and the conductivity was recorded using the oscilloscope (Fig. 5). The conductivity was measured both on the way through the flame and on the return, and the latter was found to be consistently smaller in a constant ratio. This is probably because of a lower conductivity in the wake of the receding probe. Since the probe was of nonnegligible diameter compared to the flame thickness, no conclusive determination of conductivity gradients within the flame could be inferred.

In order to determine the influence of mechanical motion and high temperature on the probe response, several runs were made without seeding the flame. No signal was detected on the most sensitive scale during the traverse time.

The flame conductivity was measured for NaCl, KCl, RbCl, and CsCl as a function of the normality of the seeding solution. The seeding solutions were prepared and checked, using known electrolytic conductivity data, against values determined by immersing the probe in the electrolyte. This also served as a calibration for the probe (Fig. 6).

Constant oxygen, hydrogen, and seeding flow rates were held in order to retain constant flame conditions. The seeding rate was determined by weighing the atomizer and leads before and after a run of known duration. The flow

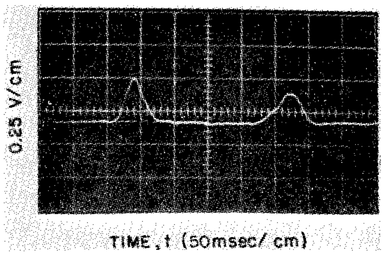

Fig. 5 Conductivity output signal.

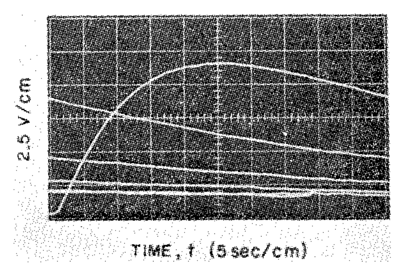

Fig. 4 Probe thermal response.

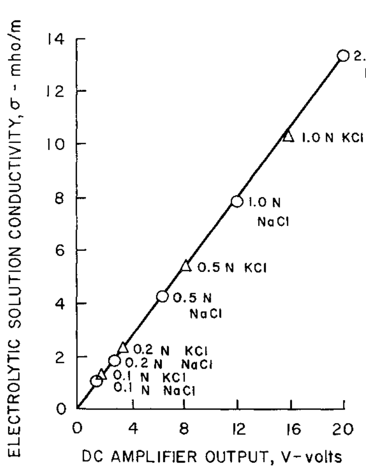

Fig. 6 Probe calibration curve.

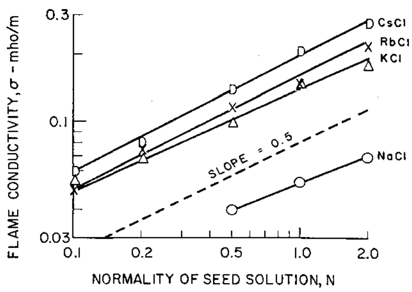

Fig. 7 Flame conductivity data.

rates of O_2, H_2, and Cs were measured to be 0.62, 1.00, and 3.0×10^{-4} mole/min. (The seeding solution also added 8.3×10^{-3} and 3.0×10^{-4} mole/min of H_2O and Cl, respectively, to the combustion products.) The concentration of Cs in the flame was therefore $7.5 \times 10^{14}/\text{cm}^3$.

It is to be expected that the alkali content is divided in some way among the salt form (including droplets of the solution which might not completely evaporate), molecular and atomic forms, and ionized state. The latter state is the principal contributor to the electron concentration of the flame, which is in turn proportional to the electrical conductivity. A competing mechanism is the attachment of electrons to OH, Cl, and other electronegatives, rendering a portion of the electrons unavailable for the conduction of current. Thus, conductivity is indicative of the number of free electrons and is, in fact, a measure of this quantity if the electron collision frequency is known.

The dependence of the measured flame conductivity on normality of the seeding solution, shown in Fig. 7, exhibits the general behavior expected of a gas in thermodynamic equilibrium. In particular, the data verify the simple form of the Saha equation for low electron concentrations in a plasma, that is, $n_e = n_s^{1/2}F_s^{1/2}(V_s,T)$, where n_e and n_s are the electron and total alkali concentrations and $F_s(V_s,T)$ is a function depending only upon gas temperature T and the ionization potential V_s of the alkali. The linear correspondence of conductivity to the one-half power of normality is evident in Fig. 7. Moreover, $F_s^{1/2}(V_s,T)$ is an exponentially decreasing function of ionization potential whose general form of $e^{-eV_s/2kT}$ is qualitatively verified by the spacing of the curves for various seeding materials.

Microwave transmission diagnostics in the range of 70 to 90 kMc/sec were employed to obtain an independent measurement of electron density in the flame, to serve as a basis for comparison with the conductivity data obtained with the probe. An approximate measure of the product of electron density and collision frequency was obtained using the method of Belcher and Sugden,[3] that is, by detecting the attenuation coefficient. Horns with dielectric lenses were used to focus the microwave radiation through the flame center at 3 in. above the burner, and the attenuation was measured.

A great deal of scatter occurred in the microwave data, the largest divergence from the mean value being about 50%. A mean value of attenuation of 0.77 db/cm at 83 kMc/sec was found for the standard flame conditions employed and with a seeding solution of 2N CsCl. According to the theory of Ref. 3, this corresponds to an electron density of $2.2 \times 10^{12}/\text{cm}^3$ if the collision frequency is taken to be $2.6 \times 10^{11}/\text{sec}$.[5] These values correspond in turn to a d.c. conductivity of 0.24 mho/m, whereas the value measured by the probe under the same flame conditions is 0.27 mho/m. Although this agreement is perhaps fortuitous, the value of conductivity obtained from the microwave measurements is probably in error, due to scatter in the data and uncertainty in the flame diameter, by no more than a factor of 2.

Values of electron density were calculated using the Saha equation and compared with values obtained from the conductivity probe data using $\sigma = n_e e^2/m\nu_c$, where $e = 1.6 \times 10^{-19}$ coul, $m = 9.1 \times 10^{-31}$ kg, and $\nu_c = 2.6 \times 10^{11}\ \text{sec}^{-1}$. The Saha equation predicted, in the case of each seeding material, a considerably higher degree of ionization than was measured. This discrepancy appeared to depend on the ionization potential of the seeding agent, increasing as the ionization potential decreased. Also, the spacing of the curves for various seeding materials was less than that predicted by the Saha equation. The same effects were observed by Smith and Sugden[6] in their microwave transmission measurements of electron density in an alkali-seeded hydrogen-air flame.

It is to be expected that the value of conductivity obtained from the probe measurement should be smaller than the maximum value in the flame. This follows from the consideration that the probe is calibrated in a volume that is large in comparison with the probe coil dimensions, whereas the flame is not as thick as the full diameter over which the probe dissipates power.

The possibility of error in the conductivity probe measurements due to the existence of electrical sheaths may be discounted. Since the surface of the probe is an insulator and there is no net current from the plasma to the probe, a space-charge (Debye) sheath of approximate thickness

$$\lambda_D = (\epsilon_0 kT_e/e^2 n_e)^{1/2}$$

will surround the probe. For the conditions of the flame measurements, λ_D has a value of about 3×10^{-4} cm, whereas the distance over which the rf field interacts with the flame is of the order of 1 cm. Therefore, the effect of the sheath on the probe measurements should be insignificant. This is true also of the glow discharge data mentioned previously, where λ_D was about 10^{-2} cm.

A few conclusions that can be inferred from the preliminary conductivity probe data reported here are that a good measure of conductivity is obtained, that the conductivity increases as the one-half power of the normality of the seeding solution (as predicted by the simple form of the Saha equation), and that the most important spurious effects are eliminated except that due to the small size of the flame.

References

[1] Van Tiggelin, A., "Ion production and concentration in flames," Univ. Louvain Annual Summary Rept. 2 (May 1962).

[2] Williams, H., "The predominant process of electron decay in the mantle of an acetylene-air flame," *Seventh Symposium (International) on Combustion* (Butterworth and Co. Ltd., London, 1958), pp. 269–276.

[3] Belcher, H. and Sugden, T. M., "Studies on the ionization produced by metallic salts in flames: I. The determination of the collision frequency of electrons in coal gas/air flames," Proc. Roy. Soc. (London) **A 201,** 480–488 (1950).

[4] Lary, E. C. and Olson, R. A., "A plasma conductivity probe," *Third Symposium on Engineering Aspects of Magnetohydrodynamics* (March 1962).

[5] Schneider, J. and Hofman, F. W., "Absorption and dispersion of microwaves in flames," Phys. Rev. **116,** 244–249 (1959).

[6] Smith, H. and Sugden, T. M., "Studies on the ionization produced by metallic salts in flames: IV. The stability of gaseous alkali hydroxides in flames," Proc. Roy. Soc. (London) **A 211,** 58–74 (1952).